

Received September 22, 2020, accepted October 1, 2020, date of publication October 6, 2020, date of current version October 21, 2020.

Digital Object Identifier 10.1109/ACCESS.2020.3028765

Research on Optical Fiber Sensor Localization Based on the Partial Discharge Ultrasonic Characteristics in Long-Distance XLPE Cables

ZHIHENG LIU^{1,3}, XIULING LIU¹, ZHAOYAN ZHANG¹, WENNA ZHANG², AND JIANQUAN YAO³

¹College of Electronic Information Engineering, Hebei University, Baoding 071002, China

²Yuncheng Power Supply Company, State Grid Shanxi Electric Power Company, Yuncheng 044000, China

³Key Laboratory of Opto-electronic Information Technology, Ministry of Education, Tianjin University, Tianjin 300072, China

Corresponding author: Xiuling Liu (liuxiuling17@126.com)

This work was supported in part by the Foundation of Hebei Education Department under Grant QN2019202, in part by the Foundation of President of Hebei University under Grant XZJJ201908, and in part by the Hebei University One Province One University Special Fund under Grant 801260201232.

ABSTRACT To improve the safety and antielectromagnetic interference performance of partial discharge detection in high-voltage DC cables, partial discharge of cables is used as a criterion for characterizing insulation defects. An ultrasonic detection method for the partial discharge of optical fiber detection is carried out in a long-distance high-voltage DC operating environment. By analyzing the partial discharge mechanism and ultrasonic characteristics of DC cables, a correlation model between partial discharge ultrasonic waves and discharge quantity is established. The partial discharge charge of several common insulation defects is obtained experimentally, and an ultrasonic characteristic Sagnac fiber detection system is realized. Standard ultrasonic time domain signal detection and fiber-optic sensing probe directional experiments are performed. The influence of fiber sensing probes with different lengths on the sensitivity of partial discharge signals is investigated based on the frequency distribution characteristics of partial discharges. The ultrasonic wave is measured based on a fiber-optic probe and can perform multipoint detection, and the partial discharge of the ± 320 kV flexible DC transmission system was tested based on the developed optical fiber sensing system. The experimental results show that the partial discharge signal detection of 6 km long cable can be realized, and the localization accuracy is less than ± 80 m. It provides a practical monitoring method for the perception of long-distance transmission equipment operating states.


INDEX TERMS HVDC cable, partial discharge, Sagnac fiber sensing, delay fiber, localization algorithm.

I. INTRODUCTION

The insulation medium of DC cables and accessories suffers from high-intensity local electric fields, polarity reversal voltages and nonlinear temperature characteristics caused by space charge accumulation during power transmission [1]. In turn, partial discharges are triggered, and discharge channels are easily formed, resulting in breakdowns of insulating material. Partial discharge (PD) measurement is an effective method to evaluate the operating conditions of high-voltage DC cables and accessories [2].

In recent years, DC power transmission systems have been commissioned with higher rated voltages and longer distances [3], [4]. Predecessors have done some analysis

in the propagation characteristics of cable PD signals, which include a three-dimensional simulation model of cable joints [5]. A measurement of partial discharge (PD) phenomena and clustering in the defect pattern of a cross-linked polyethylene power cable joint was discussed [6]. The experimental investigation of two PD defects/sources at different locations on a medium voltage (MV) cable section was presented [7]. The PD characteristics of a single source or multiple sources of DC XLPE cables were obtained from two different frequency bands by detecting the frequency response of the antenna [8], and the partial discharge patterns were distinguished based on image features [9]. A numerical model that describes the partial discharge characteristics of high-voltage direct-current HVDC cables was built considering the effects of the electric field and charge dynamics [10], and the partial discharge position was determined by

The associate editor coordinating the review of this manuscript and approving it for publication was Arpan Kumar Pradhan .

analyzing the time and angle information of UHF electromagnetic waves generated by partial discharge [11]. A new approach was proposed based on the discrete wavelet transform for detecting insulated overhead conductor faults according to partial discharge [12], which achieves the identification and classification of different types of events, including internal PD, corona PD, surface PD, and noise [13]. However, the specific localization algorithm requires large sensor hardware overhead and is difficult to apply.

Ultrawideband fiber-optic acoustic sensors, with small size, low cost, and high sensitivity, have been rapidly developed [14], [15] and are used in the partial discharge detection of DC cables and accessories. The Fabry-Perot interferometer (EFPI) ultrasonic sensor [16] has been experimentally verified to have a minimum detectable ultrasonic pressure from 1.5 mPa/sqrt (Hz) to 0.625 mPa/sqrt (Hz) between 20 kHz and 40 kHz. Taiyuan University of Technology used optical fiber sensing and time-frequency analysis of ultrasonic signals excited by piezoelectric ultrasonic transducers to detect partial discharges in power cables [17]. A fiber Fabry-Perot (FP) interferometer integrated with the adaptive fiber ring laser was configured as a switchable multiwavelength fiber laser, which can be used to detect the ultrasonic signal of the discharge source with a variable incidence angle and linear distance [18]. Partial discharge detection and localization of the cable was realized by calculating the possible deviation in the measurement of the acoustic emission sensor to compensate for the measurement noise caused by the aging of the sensor or the environment [19], [20]. A 10 kV oscillating wave system was built based on the wavelet transform modulus maximum method and related methods in the laboratory by the State Grid Corporation and North China Electric Power University [21], [22]. The system was used to perform partial discharge detection in a 497 m defective cable and analyze the influence of the wave speed characteristics of the cable on the localization accuracy of short-distance cables. A zero-drift delay compensation model for a fiber ring was established by studying the zero-drift delay response characteristics caused by the nonreciprocal phase error in the thermal diffusion of the fiber ring in a fiber optic gyroscope [23]. An FPGA-based polarization control method was proposed by Tianjin University [24], which integrated polarization controller feedback technology, FPGA hardware parallel structure and pipeline technology to quickly implement algorithm iteration and control the polarization controller to adjust the polarization state. A partial discharge detection and localization system for high voltage cable based on a long-tailed optical fiber Sagnac interferometer has been proposed and the experimental results show that the accuracy of partial discharge localization is 0.016 km [25].

These researchers carried out in-depth research on the suppression of polarization phase shift and polarization-induced signal fading by the optical fiber sensor localization detection system from the above analysis. There is still a lack of experimental research on the distributed multipoint detection of long-distance DC cables, the synchronous demodulation

of PD signals, and the optical fiber localization detection of partial discharge points.

In this paper, we first analyze the mechanism of the effect of delay fiber length on the sensitivity of the partial discharge ultrasonic characteristics optical fiber sensor detection system based on Sagnac sensing technology and verify it through experiments. Second, we analyze the localization principle and localization algorithm based on the double-loop Sagnac interference partial discharge localization. Finally, an experimental verification is carried out with fiber optic detection of the partial discharge ultrasonic characteristics for a DC cable in a 320 kV DC system.

II. SENSITIVITY ANALYSIS OF THE OPTICAL FIBER SENSING SYSTEM

A partial discharge ultrasonic characteristic optical fiber sensing detection system was built based on Sagnac sensing technology and includes an interference-type Sagnac optical fiber sensing system, a host computer acquisition system and a partial discharge simulation device, as shown in Fig. 1.

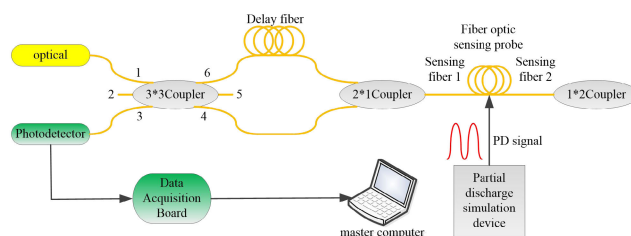


FIGURE 1. Partial discharge ultrasonic characteristic optical fiber sensing detection system.

The ultrasonic waves generated by different insulation defects under the same detection model are different, and the attenuation rate of the ultrasonic amplitude in the medium is different according to the transmission characteristics of the partial discharge ultrasonic wave of the cable. The two beams of light in the Sagnac interferometer are transmitted in opposite directions. There is an optical path difference when the light passes through the same position of the sensing fiber due to the delay fiber. The optical path difference and the total optical path in the interference loop change proportionally when a partial discharge occurs in the cable, which causes changes in phase and optical power.

According to the principle of light interference, there are two optical path loops in the optical fiber sensing detection system that interfere at the 3×3 coupler to form an interference loop. Two beams of coherent light pass through the optical fiber sensing probe successively, and the modulation of the partial discharge signal on the two beams of light causes the phase of the two beams to change, and the phase change is converted into a change in light intensity. The optical signal carrying the partial discharge signal is converted into an electric signal carrying the partial discharge signal through the photodetector, and the electric signal is collected and

analyzed through the data acquisition module, and finally the output signal is displayed by the upper computer.

We focused on the analysis of the mechanism of delay fiber on the sensitivity of partial discharge detection, which is an important factor affecting detection sensitivity.

A. ANALYSIS OF THE MECHANISM OF THE EFFECT OF DELAY FIBER LENGTH ON SENSITIVITY

The partial discharge signal of the DC cable can be set as $y(t) = A_0 \sin(\omega_0 t + \varphi_0)$. The partial discharge signal is a continuous small signal, and the i -th signal can be expressed as $y(t) = \sum A_i \sin(\omega_i t + \varphi_i)$. The phase change of the two forward and backward optical paths through the delay fiber caused by the partial discharge signal in a single pass can be expressed as:

$$y_1(t) = \sum_{i=1}^N A_i \{ \sin[\omega_i(t-t_a)t + \varphi_i] - \sin[\omega_i(t-t_b)t + \varphi_i] \} \tag{1}$$

$$y_2(t) = \sum_{i=1}^N A_i \{ \sin[\omega_i(t-t_c)t + \varphi_i] - \sin[\omega_i(t-t_d)t + \varphi_i] \} \tag{2}$$

where $t_b = (2L_2 + L_1)n/c$, $t_c = L_1n/c$, and $t_d = (L_D + L_1 + 2L_2)n/c$. The phase difference between the forward and backward beam paths is:

$$\Delta y(t) = y_1(t) - y_2(t) = 4 \sum_{i=1}^N \left\{ A_i \sin(\omega_i \frac{L_D n}{2c}) \cos\left(\omega_i \frac{L_2 n}{c}\right) \times \cos\left[\omega_i \left(t - \frac{(L_D + 2L)n}{c}\right) + \varphi_i\right] \right\} \tag{3}$$

where $L = L_1 + L_2$, $t_a = (L_D + L_1)n/c$, $\hat{A} \sin\left(\omega_i \frac{L_D n}{2c}\right) = 0$, $\omega_i = \frac{2k\pi c}{L_D n}$, $\omega_i = 2\pi f_i$. The relationship between the delay fiber and the frequency of the partial discharge signal is $f_i = \frac{kc}{nL_D}$. n is the fiber index, and c is the speed of light in a vacuum. It can be seen from the above formula that the frequency of the partial discharge signal f is inversely proportional to the length of the delay fiber L_D within a certain range. It provides a theoretical basis for studying the relationship between the sensitivity of the fiber-optic sensing of the partial discharge of the DC cable and the length change in the delay fiber.

B. EXPERIMENT AND ANALYSIS OF DELAY FIBER SENSITIVITY

The length of the delay fiber was changed to perform sensitivity experiments according to the system diagram shown in Figure 1. The sensor fiber is wound into a fiber-optic sensor probe with a diameter of 10 cm; the total length of the sensor probe fiber is 50 m, and the sensing fiber length is 2 km at the beginning of the interference-type Sagnac fiber-optic sensor partial discharge detection system. We acquired the results,

as shown in Table 1, from repeat tests with a delay fiber of the different length.

TABLE 1. The data of the partial discharge detection system with different length delay fibers.

Delay fiber length/km	Input optical power/mW	Time domain signal amplitude/mV	Center frequency/kHz	Center frequency intensity/dB
2.012	10.01	10	7.58	140.1
4.050	10.01	20	7.50	346.6
6.192	10.01	17.78	7.50	264.2
12.352	10.01	22.76	6.96	594.5
14.316	10.01	15.55	6.93	582
18.318	10.01	18.32	6.94	579.2
26.668	10.01	11.55	6.95	351.6

According to Table 1, the variation curve of the central frequency and the central frequency intensity of the partial discharge frequency domain collected by the partial discharge detection system based on the Sagnac optical fiber sensing technology under different lengths of delay fiber is drawn, and the statistical results are shown in Fig. 2.

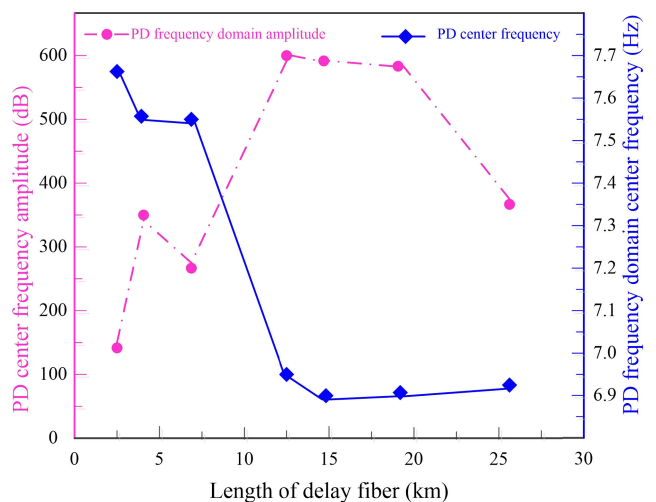


FIGURE 2. The variation curve of the partial discharge frequency domain signal with the length of the delay fiber.

The center frequency of the partial discharge frequency domain signal changes with the length of the delay fiber. When the length of the sensing fiber is 2 km, the other test conditions remain unchanged. The center frequency of the partial discharge frequency domain decreases with the length of the delay fiber when the length of the delay fiber ranges from 2 km to 12.352 km. The center frequency of the partial discharge frequency domain signal tends to a constant value

of 6.95 kHz when the length of the delay fiber is greater than 14.316 km. The amplitude of the partial discharge center frequency also changes with the length of the delay fiber. The center frequency intensity of the partial discharge frequency domain signal has a maximum value when the length of the delay fiber is approximately 12 to 18 km.

The frequency characteristics of the 110 sets of partial discharge signals collected by the system were studied, and the spectrum of partial discharge signals was obtained by fast Fourier transform, as shown in Fig. 3.

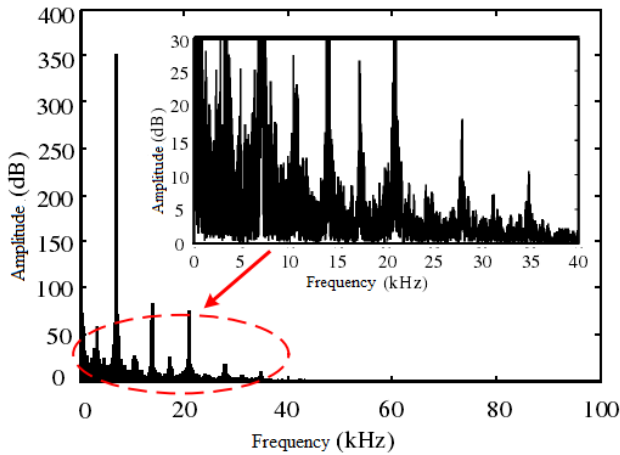


FIGURE 3. Frequency domain diagram of the partial discharge signal.

The frequency domain waveform interval of the partial discharge signal ranges from 6 kHz to 40 kHz, and its center frequency is 7 kHz. Therefore, this experimental scheme can identify and detect the partial discharge signal. There was changing in the length of the delay fiber form 2.5km to 27.5km, and the length of the sensing fiber was set to 0.5 km. Then, we repeatedly obtained the amplitude of the time domain signal from the above test. The experimental statistical results are shown in Figure 4 by collecting and averaging the data of repeated experiments on the same length of delay fiber.

In Fig. 4, it can be seen that the length of the delay fiber is different and the amplitude of the time-domain signal for the partial discharge signal is different. For the sensing fiber of different lengths, the time-domain signal amplitude of the partial discharge signal has a similar trend. When the delay fiber length is approximately 12.352 km, the sensitivity of the sensing probe to the partial discharge signal time domain response is higher under different lengths of sensing fiber.

III. THE PARTIAL DISCHARGE OF CABLE BASED ON OPTICAL FIBER SENSOR LOCALIZATION DETECTION

A. THE LOCALIZATION PRINCIPLE OF A DOUBLE-LOOP SAGNAC INTERFERENCE-TYPE FIBER

The experimental principle diagram of the partial discharge detection and positioning of the cable based on the double-loop Sagnac interference optical fiber sensing partial discharge ultrasonic characteristic detection system is shown

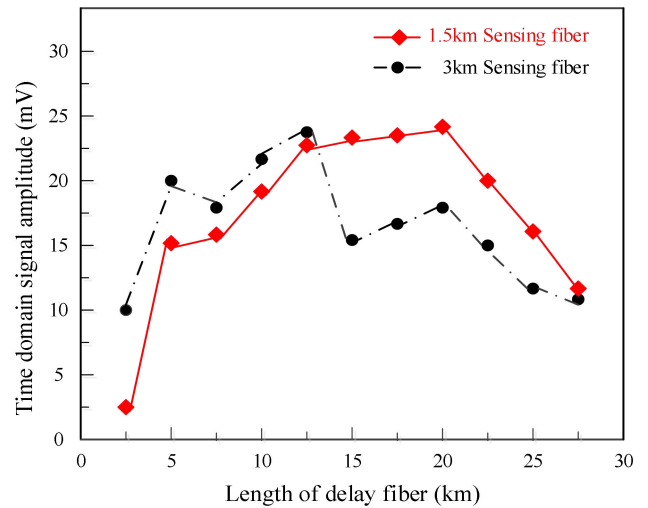


FIGURE 4. The curve of the partial discharge time-domain signal with the length of the delay fiber.

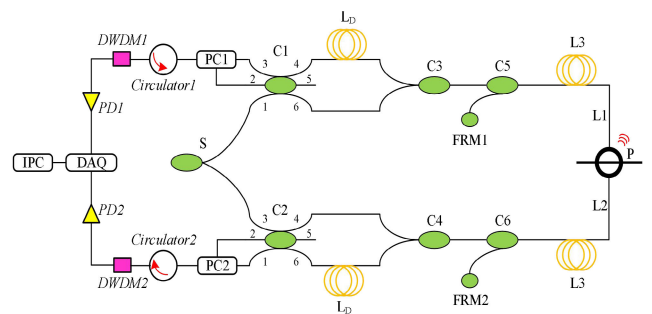


FIGURE 5. Partial discharge detection system diagram for double-loop Sagnac interference-type optical fiber sensing.

in Fig 5. The light emitted by the light source is divided into two beams of equal light intensity through the coupler C, and there are four light paths passing through C1. The optical path can be interfered when the light has gone through the delay fiber LD based on the interference theorem.

- Path1: S-C1-Ld-C3-L3-P-L3-FRM2-L3-P-L3-C3-C1;
 - Path2: S-C1-C3-L3-P-L3-FRM2-L3-P-L3-C3-Ld-C1;
 - Path3: S-C1-C3-L3-P-L3-FRM2-L3-P-L3-C3-C1;
 - Path4: S-C1-Ld-C3-L3-P-L3-FRM2-L3-P-L3-C3-Ld-C1;
- DAQ, Data Acquisition Card; IPC, Industrial Personal Computer; PD1, PD2, Photo-detector; DWDM1, DWDM2, Dense Wavelength Division; Circulator1, Circulator2, Optical Circulator; PC1, PC2, Polarization Controller; C1, C2, C3, C4, C5, C6, Split Coupler; FRM1, FRM2, Faraday Rotating Mirror; LD, Delay Fiber; L3, Guide Fiber; P, Partial Discharge Signal

The phase of the two beams of light will change because of the influence of the partial discharge signal in the cable. The expressions of the first two optical paths can be set as P1 and P2:

$$P_1 = P_0 \exp \{j[\omega_c t + \psi(t - \tau_1) + \psi(t - \tau_2) + \varphi_1]\} \quad (4)$$

$$P_2 = P_0 \exp \{j[\omega_c t + \psi(t - \tau_3) + \psi(t - \tau_4) + \varphi_2]\} \quad (5)$$

The amplitude of the two beams is equal to P_0 under the condition of ideal splitting of the coupler. φ_1 and φ_2 represent the initial phase of the two beams, and ω_c represents the angular frequency of light waves. The phase change of the first beam of coherent light affected by the partial discharge ultrasonic signal is $\psi(t - \tau_1)$ and $\psi(t - \tau_2)$ at the moments of $t - \tau_1$ and $t - \tau_2$, respectively. The phase change of the first beam of coherent light affected by the partial discharge ultrasonic signal is $\psi(t - \tau_3)$ and $\psi(t - \tau_4)$ at the moment of $t - \tau_3$ and $t - \tau_4$, respectively, where $\tau_1, \tau_2, \tau_3, \tau_4$ can be expressed as:

$$\begin{aligned}\tau_1 &= \frac{n(L_1 + L_3)}{c}; \\ \tau_2 &= \frac{n[L_1 + L_3 + 2(L_2 + L_3)]}{c}; \\ \tau_3 &= \frac{n(L_1 + L_3 + L_D)}{c}; \\ \tau_4 &= \frac{n[L_1 + L_3 + 2(L_2 + L_3)]}{c};\end{aligned}$$

where L_1 is the distance from the guiding fiber to the partial discharge point P, L_2 is the distance from P to L_3 , n is the refractive index of the fiber, and c is the speed of light propagating in a vacuum. The interference communication items of the two beams are:

$$I_{12} = P_0^2 \cos[\Delta\psi_1(t) + \varphi_1 - \varphi_2] \quad (6)$$

The total phase change caused by the partial discharge signal can be expressed as $\Delta\psi_1(t)$.

$$\Delta\psi_1(t) = \psi(t - \tau_1) + \psi(t - \tau_2) - \psi(t - \tau_3) - \psi(t - \tau_4) \quad (7)$$

The localization function is expressed as:

$$\theta(t) = \psi(t) - \psi\left(t - \frac{nL_D}{c}\right) \quad (8)$$

Therefore,

$$\begin{aligned}\Delta\psi_1(t) &= \theta\left[t - \frac{n(L_2 + L_3)}{c}\right] \\ &\quad + \theta\left[t - \frac{n(L_1 + L_3)}{c} - \frac{2n(L_2 + L_3)}{c}\right] \\ \Delta\psi_2(t) &= \theta\left[t - \frac{n(L_2 + L_3)}{c}\right] \\ &\quad + \theta\left[t - \frac{n(L_2 + L_3)}{c} - \frac{2n(L_1 + L_3)}{c}\right]\end{aligned}$$

$\Delta\psi_1(t)$ and $\Delta\psi_2(t)$ are two signals related to t , of which the signal indicated by the first item arrives before the second item by at least $2nL_3/c$. The following relationship can express the time difference of $\Delta\psi_1(t)$ and $\Delta\psi_2(t)$ as:

$$\begin{aligned}\Delta\tau &= \frac{n(L_1 - L_2)}{c}, \text{ there, } L = L_1 + L_2, \text{ so} \\ L_1 &= \frac{L + \Delta\tau \cdot c/n}{2}\end{aligned} \quad (9)$$

B. DOUBLE-LOOP SAGNAC INTERFEROMETRIC FIBER-OPTIC SENSING PARTIAL DISCHARGE LOCALIZATION ALGORITHM

The sampling signals of photodetectors 1 and 2 can be expressed as: $x(n) = \alpha_1 s(n) + n_1(n)$,

$$y(n) = \alpha_2 s(n - \Delta\tau) + n_2(n)$$

where α_1 and α_2 are conversion factors for the two photodetectors, $n_1(n)$ and $n_2(n)$ are interference noise in the fiber-optic sensing system, and $\Delta\tau$ is the time delay between the two signals. We can obtain the time delay based on the cross-correlation function between the two signals and achieve the localization of the partial discharge signal.

$$\begin{aligned}R_{xy}(m) &= \sum_{n=0}^{N-1} x(n-m)y(n) \\ &= \alpha_1\alpha_2 \sum_{n=0}^{N-1} [s(n) + n_1(n)][s(n-m-\Delta\tau) + n_2(n)]\end{aligned} \quad (10)$$

It can be considered that $s(t)$, $n_1(n)$ and $n_2(n)$ are not related to each other when the noise signal is much smaller than the partial discharge signal. Then, formula (10) can be simplified as $R_{xy}(m) = \alpha_1\alpha_2 \sum_{n=0}^{N-1} s(n)s(n-\Delta\tau-m)$, where the offset of the peak abscissa of the function from zero reflects the delay between the two signals. When the sampling rate is f_s , the delay can be expressed as $\Delta\tau = \frac{\arg \max[R_{xy}(m)]}{f_s}$, and the localization where the partial discharge point occurs can be obtained by formula (9) according to the calculation result of the delay.

IV. EXPERIMENTAL VERIFICATION OF PARTIAL DISCHARGE OPTICAL FIBER SENSING FOR HVDC CABLES

To verify the feasibility of detecting the insulation defects of XLPE HVDC cables under DC voltage, a test cable loop was constructed using the same batch of 320 kV HVDC XLPE cables that were used to build the ± 320 kV VSC-HVDC project. The total length of the transmission line is 15.7km, all of which are land cables.

The DC cable in the ± 320 kV flexible DC transmission system was selected for the field test. The cross-sectional area of the cable is 1800 mm², and the rated voltage is ± 320 kV. A schematic diagram of DC cable partial discharge detection wiring is shown in Fig. 6.

A certain section of cable in the transmission line has been implemented with artificial insulation defects, which is causing partial discharge during high-voltage transmission. The experimental platform for constructing a dual-loop Sagnac interference partial discharge detection system is shown in Fig. 7. A piezoelectric transducer (PZT) is used to simulate ultra-acoustic signal of high voltage cable partial discharge. The partial discharge signal generation and data acquisition of high-voltage DC cables are shown in Fig. 8, and partial discharge detection and localization experiments are carried out.

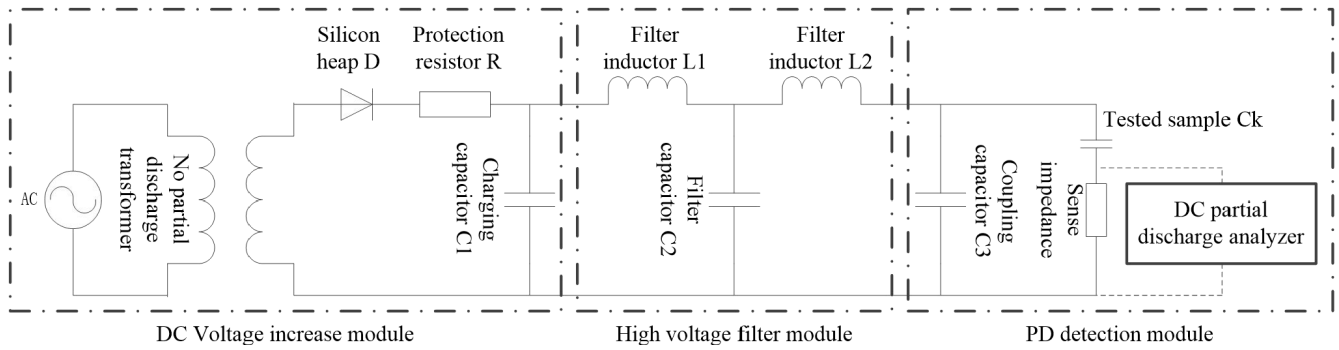


FIGURE 6. Schematic diagram of DC cable partial discharge detection wiring.

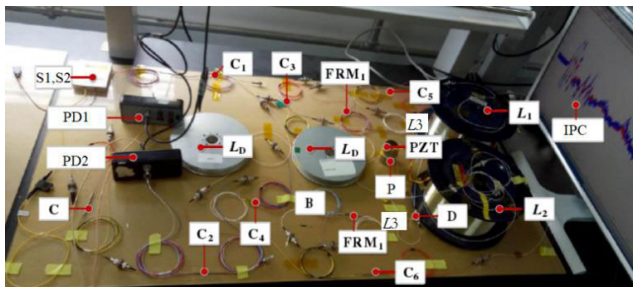


FIGURE 7. Experimental platform of dual-circuit Sagnac interference partial discharge detection.

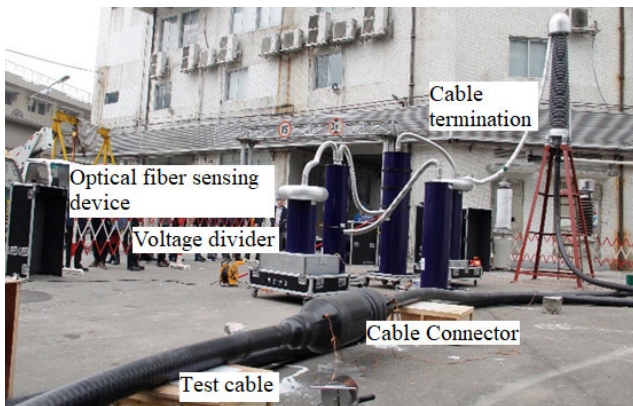


FIGURE 8. Partial discharge signal generation and data acquisition of high-voltage DC cables.

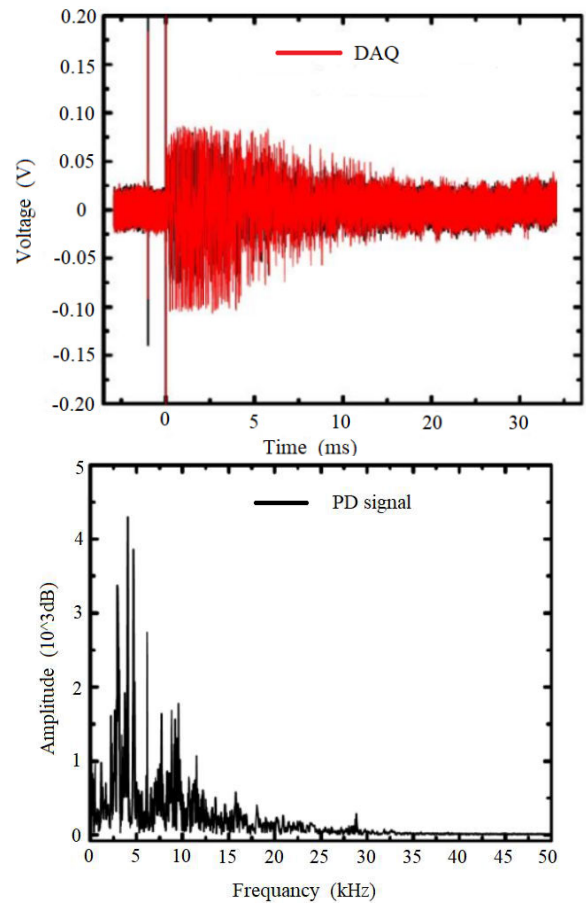


FIGURE 9. Dual-loop Sagnac detected partial discharge signal time and frequency domain signal.

A high-voltage AC transformer is converted into a DC high-voltage output through a silicon stack rectification method in this paper, which has less high-frequency interference and is suitable for the measurement of DC partial discharge phenomena. The model of the high-voltage AC transformer is YDTW-50/150, the rated voltage is 150/0.38kV, and the rated capacity is 50kVA; the parameters of the rectifier silicon stack are 600kV, 100mA; the partial discharge of the DC high-voltage output module less than 5pC at the rated voltage.

The parameters of the optical fiber sensor detection system were set as follows: the length of the delay fiber was 4 km,

the length of the guide fiber was 2 km, the length of the sensing fiber was 9.25 km, and the sampling rate of the high-speed data acquisition card was 80 MHz.

The optical fiber sensing system is used to detect the partial discharge of the insulation defects applied at 6 km on the cable, and the time domain and frequency domain waveforms of the partial discharge signals collected by the photo-detector are shown in Fig. 9. It can be seen that the

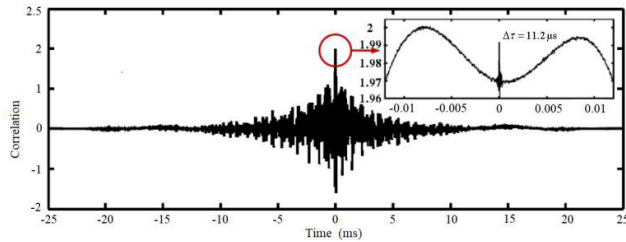


FIGURE 10. Cross-correlation curve of two-channel photodetector signals.

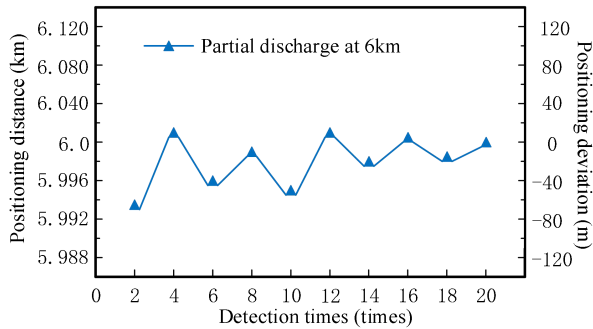


FIGURE 11. Statistics of the localization results of the partial discharge signal of the DC cable.

amplitude of the time domain signal is 0.1 V, the decay time is 10 ms, the frequency is concentrated within 30 kHz, and the detection frequency range is relatively narrow, which is suitable for the detection of the partial discharge signal on the DC cable.

The results for the cross-correlation processing of the two-channel photo-detector signals are shown in Fig. 10, and the upper right corner shows a partially enlarged display of the cross-correlation function. The delay response of the peak abscissa is $\Delta\tau = 11.2\mu\text{s}$, which is located on the left side of the zero axis. The vibration point distance is $L_1 = 5.94\text{ km}$ based on the calculation of the localization formula, and the localization error is $\pm 60\text{ m}$.

The above experimental process is repeated to perform a statistical analysis on the localization results of the partial discharge signal of the DC cable, as shown in Fig. 11. The localization position is mainly concentrated within 6 km, and the localization error is approximately $\pm 100\text{ m}$, which shows that the localization error is not affected by the frequency.

According to theoretical analysis and the experimental results, the localization accuracy of the dual-loop Sagnac interferometric partial discharge ultrasonic characteristic optical fiber sensor detection system can range within $\pm 80\text{ m}$. According to the statistics from multiple experimental results, the localization errors have low dispersion.

V. CONCLUSION

The mechanism of the influence of the delay fiber on the detection sensitivity is analyzed theoretically and experimentally; the amplitude of the partial discharge time domain signal detected by the system when the length of the delay

fiber is 12.3 km is the highest, and the center frequency of the frequency domain signal is the highest. A dual-loop Sagnac interference-type optical fiber sensor partial discharge detection system was established, and the cable partial discharge localization algorithm based on the cross-correlation of the interference signals in the system was clarified. An experimental test was carried out on the partial discharge of the DC cable in a $\pm 320\text{ kV}$ flexible DC transmission system. The experimental results show that the optical fiber sensing system can realize the partial discharge signal detection for a 6 km long-distance cable, and the localization accuracy can reach $\pm 80\text{ m}$. The effectiveness of the fiber-optic sensing system in cable condition monitoring applications is verified, which provides a practical monitoring method for the perception of long-distance transmission equipment operating states.

REFERENCES

- [1] Y.-P. Xu, F.-Y. Yang, and Y. Qian, "Pattern recognition of PD in DC cable terminal joint based on the improved ECOC Classifier," *Proc. CSEE*, vol. 37, no. 4, pp. 1260–1268, Feb. 2017.
- [2] P. Romano, G. Presti, A. Imburgia, and R. Candela, "A new approach to partial discharge detection under DC voltage," *IEEE Elect. Insul. Mag.*, vol. 34, no. 4, pp. 32–41, Jul. 2018.
- [3] X. Gu, S. He, Y. Xu, Y. Yan, S. Hou, and M. Fu, "Partial discharge detection on 320 kV VSC-HVDC XLPE cable with artificial defects under DC voltage," *IEEE Trans. Dielectr. Electr. Insul.*, vol. 25, no. 3, pp. 939–946, Jun. 2018.
- [4] F. Barakou, P. A. A. F. Wouters, S. Mousavi-Gargari, J. P. W. de Jong, and E. F. Steennis, "Online transient measurements of EHV cable system and model validation," *IEEE Trans. Power Del.*, vol. 34, no. 2, pp. 532–541, Apr. 2019.
- [5] Y. Zhou, Y. Wang, and W. Wang, "A study on the propagation characteristics of partial discharge in cable joints based on the FDTD method," *IEEE Access*, vol. 8, pp. 130094–130103, 2020.
- [6] F.-C. Gu, H.-T. Yau, and H.-C. Chen, "Application of chaos synchronization technique and pattern clustering for diagnosis analysis of partial discharge in power cables," *IEEE Access*, vol. 7, pp. 76185–76193, May 2019.
- [7] M. Shafiq, I. Kuitam, P. Taklaja, L. Kutt, K. Kauhaniemi, and I. Palu, "Identification and location of PD defects in medium voltage underground power cables using high frequency current transformer," *IEEE Access*, vol. 7, pp. 103608–103618, 2019.
- [8] Y. Xu, Y. Qian, F. Yang, Z. Li, G. Sheng, and X. Jiang, "DC cable feature extraction based on the PD image in the non-sampled contourlet transform domain," *IEEE Trans. Dielectr. Electr. Insul.*, vol. 25, no. 2, pp. 533–540, Apr. 2018.
- [9] Y. Xu, G. Sheng, F. Yang, X. Chen, Y. Qian, and X. Jiang, "Classification of partial discharge images within DC XLPE cables in contourlet domain," *IEEE Trans. Dielectr. Electr. Insul.*, vol. 25, no. 2, pp. 486–493, Apr. 2018.
- [10] M. A. Fard, M. E. Farrag, S. McMeekin, and A. Reid, "Electrical treeing in cable insulation under different HVDC operational conditions," *Energies*, vol. 11, no. 9, pp. 2405–2419, Sep. 2018.
- [11] M. He, M. Hao, G. Chen, X. Chen, W. Li, C. Zhang, H. Wang, M. Zhou, and X. Lei, "Numerical modelling on partial discharge in HVDC XLPE cable," *Compel Int. J. Comput. Math. Electr. Electron. Eng.*, vol. 37, no. 2, pp. 986–999, Mar. 2018.
- [12] Q. Che, H. Wen, X. Li, Z. Peng, and K. P. Chen, "Partial discharge recognition based on optical fiber distributed acoustic sensing and a convolutional neural network," *IEEE Access*, vol. 7, pp. 101758–101764, Jul. 2019.
- [13] N. Qu, Z. Li, J. Zuo, and J. Chen, "Fault detection on insulated overhead conductors based on DWT-LSTM and partial discharge," *IEEE Access*, vol. 8, pp. 87060–87070, 2020.
- [14] Zh. Li, L. G. Luo, J. D. Chen, "Novel localization method for partial discharge based on ultra-high frequency wireless sensor array," *High Voltage Eng.*, vol. 45, no. 2, pp. 88–95, Feb. 2019.

- [15] X. Guo, J. Zhou, C. Du, and X. Wang, "Highly sensitive miniature all-silica fiber tip Fabry-Pérot pressure sensor," *IEEE Photon. Technol. Lett.*, vol. 31, no. 9, pp. 689–692, May 1, 2019.
- [16] W. J. Ni, P. Lu, X. Fu, W. Zhang, P. P. Shum, H. Sun, C. Yang, D. Liu, and J. Zhang, "Ultrathin graphene diaphragm-based extrinsic Fabry-Pérot interferometer for ultra-wideband fiber optic acoustic sensing," *Opt. Express*, vol. 26, no. 16, pp. 20758–20767, Aug. 2018.
- [17] T. G. Liu, Z. Yu, and J. F. Jiang, "Advances of some critical technologies in discrete and distributed optical fiber sensing research," *Acta Phys. Sin.*, vol. 66, no. 7, pp. 60–76, Jul. 2017.
- [18] W. Yu, X. Li, Y. Gao, H. Zhang, D. Wang, and B. Jin, "Partial discharge ultrasound detection using the sagnac interferometer system," *Sensors*, vol. 18, no. 5, pp. 1425–1433, May 2018.
- [19] W. R. Si, C. Fu, D. Li, H. Li, P. Yuan, and Y. Yu, "Directional sensitivity of a MEMS-based fiber-optic extrinsic Fabry-Pérot ultrasonic sensor for partial discharge detection," *Sensors*, vol. 18, no. 6, pp. 1975–1984, Jun. 2018.
- [20] H. M. Wei and S. Krishnaswamy, "Adaptive fiber-ring lasers based on an optical fiber Fabry-Pérot cavity for high-frequency dynamic strain sensing," *Appl. Opt.*, vol. 59, no. 2, pp. 530–535, Feb. 2020.
- [21] W. M. F. Al-Masri, M. F. Abdel-Hafez, and A. H. El-Hag, "Toward high-accuracy estimation of partial discharge location," *IEEE Trans. Instrum. Meas.*, vol. 65, no. 9, pp. 2145–2153, Sep. 2016.
- [22] G. Shuguo, L. Hechen, F. Hui, P. Shaotong, L. Yungpeng, P. Jin, and W. Zhilu, "PD location method of power cable based on wavelet transform modulus maxima considering wave characteristics," *Power Syst. Technol.*, vol. 40, no. 7, pp. 2244–2250, Jul. 2016.
- [23] H. Yan, Y. H. Yang, and F. L. Yang, "Response model and compensation technology of thermal diffusion delay in fiber optic gyro coil," *Chin. J. Lasers*, vol. 2019, no. 1, pp. 255–261, Jan. 2019.
- [24] P. Ch Li *et al.*, "Research on polarization control of distributed optical fiber sensing system based on FPGA," *Chin. J. Lasers*, vol. 45, no. 5, pp. 229–235, May 2018.
- [25] Z. Song, M. Guo, and Q. Wang, "A partial discharge detection and localization system for high voltage cable based on long-tailed sagnac interferometric fiber optic sensor," *Microw. Opt. Technol. Lett.*, vol. 59, no. 9, pp. 2132–2136, Sep. 2017.



ZHIHENG LIU received the M.S. degree in electric machines and electric apparatus from the Taiyuan University of Technology, Taiyuan, China, in 2011, and the Ph.D. degree in electric machines and electric apparatus from the Dalian University of Technology, Dalian, China, in 2017.

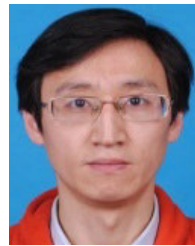
He is currently a Postdoctoral Fellow in photoelectric engineering with the Key Laboratory of Opto-electronic Information Technology, Ministry of Education, Tianjin University, Tianjin, China.

He is also a Lecturer with the College of Electronic Information Engineering, Hebei University, Baoding, China. His current research interests include intelligent high-voltage apparatus and intelligent testing technology, and emphasis on electrical equipment on-line detection and insulation diagnosis, advanced fiber inspection technology, and electromagnetic immunity testing technology.



XIULING LIU received the M.S. degree in power system and automation from Tianjin University, Tianjin, China, in 2002, and the Ph.D. degree from the Department of Optical Engineering, Hebei University, Baoding, China, in 2010.

She is currently a Professor with the Department of Electronic and Information Engineering, Hebei University. Her current research interests include signal processing, and emphasis on electrical equipment on-line detection and insulation diagnosis, advanced fiber inspection technology, and electromagnetic immunity testing technology.



ZHAOYAN ZHANG received the B.S. degree in computer science and technology from the College of Mathematics and Computer Science, Hebei University, Baoding, China, in 2003, and the M.S. and Ph.D. degrees in control theory and control engineering from North China Electric Power University, Baoding, in 2011 and 2017, respectively.

From 2003 to 2018, he was a Senior Engineer with Baoding SinoSimu Technology Company Ltd., Baoding. Since 2009, he has been an Associate Professor with the College of Electronic Information Engineering, Hebei University. His research interests include new energy power generation technology, power electronic converter technology, and motor speed regulation.



WENNA ZHANG received the M.S. degree in power system and automation from the Taiyuan University of Technology, Taiyuan, China, in 2011.

She was an Electrical Engineer with Yuncheng Power Supply Company, State Grid Shanxi Electric Power Company, Yuncheng, China, in 2012. Her current research interests include intelligent high-voltage apparatus and intelligent testing technology, and emphasis on electrical equipment

on-line detection and insulation diagnosis, advanced fiber inspection technology, and electromagnetic immunity testing technology.



JIANQUAN YAO is currently an Expert in laser and nonlinear optics. He is also an Academician of the Chinese Academy of Sciences. He is also a Professor with Tianjin University. He is also the Director of the Institute of Laser and Electronics. He is also an Honorary Dean of the School of Precision Instruments and Optoelectronic Engineering, Tianjin University. He developed the theory of high-power frequency-doubled laser, and invented the accurate calculation theory of the best phase matching of the biaxial crystal. It is called Yao Technology or Yao Method by the international academic community, and widely used. His research interest includes laser and nonlinear optical frequency conversion technology.

...